Computers and Concrete, Vol. 9, No. 5 (2012) 357-374
DOI: http://dx.doi.org/10.12989/cac.2012.9.5.357

Viscoelastic behaviour of non-homogeneous variable-section beams with post-poned restraints

Alessandra Fiore*, Pietro Monaco and Domenico Raffaele

Politecnico di Bari, Department of Civil and Environmental Engineering, Via Orabona 4, 70125 Bari, Italy

(Received December 21, 2009, Revised December 17, 2010, Accepted October 4, 2011)

Abstract. The aim of this paper is to develop a procedure able to calculate the long-term stress and strain patterns in modern prestressed composite structures which are largely influenced by creep and shrinkage and whose final static configuration is the result of many phases of loading and restraints conditions. The introduction of equivalent moduli, depending on the viscous and elastic features of materials, can guarantee a significant simplification of the problem presented above. The proposed calculation model has been used to design the “Quattroquercie Viaduct” located on the highway “A3” Salerno-Reggio Calabria, Italy.

Keywords: prestressed composite structures; creep; shrinkage; variation of static schemes; long term effects; equivalent moduli.

1. Introduction

Precast prestressed beams connected by a cast in-situ slab are largely applied in civil engineering, most frequently in bridges and viaducts. The long-term behaviour of these structures is the result of a complex sequence of constructive phases. In fact loads are usually applied at different times; in addition beams, often simply supported at the extremities, are joined together in order to realize a continuous structure. The subsequent increase of the degree of mutual connection between the different parts of the structure is dictated by the aim of increasing the serviceability level and the ultimate strength of the construction.

Due to the significant variability of static schemes as a result of the strains transferred with time by concrete, modern construction techniques produce a complex structural behaviour strongly depending on time (Dezi and Tarantino 1991, Dezi *et al.* 2006). The variations of structural schemes consist in the application of partial or permanent restraints (Fiore and Monaco 2009); consequently the strain state of the structure, due to loads already existing before their introduction, changes.

Moreover construction techniques involving different stages cause significant heterogeneity in the behaviour of concrete, since various structural parts or segments are constituted by concrete with different maturation age (Mola 1986, Mola 1988, Mola and Giussani 2003).

If suitable design criteria are not adopted, the just mentioned structures in the long time may be affected by large deformations and undesirable cracking (Bazant 2000). That is why it is necessary to analyze in detail the evolution of the stress-strain state of these structures and the influence of construction phases and static scheme variations.

* Corresponding author, Ph. D., E-mail: a.fiore@poliba.it

Several methods have been proposed for computing time-dependent effects in un-cracked composite sections, but they concern most of all composite steel-concrete structures (Gilbert 1989, Dezi *et al.* 2006, Gara *et al.* 2009, Kwak *et al.* 2000, Marì *et al.* 2003) or simple-spans girders (Ghali 1989). Also many efforts to analyze the cracked prestressed and reinforced concrete sections have been undertaken, with the assumption of perfect bonds between the constitutive materials (Neville *et al.* 2003, Bae *et al.* 2010). However relatively little research has been published on the time-dependent behaviour of girders which behave as simple-spans for dead loads and as continuous structures for loads applied after casting the slab (Kwak and Seo 2002).

In the present study an analytical model to predict the time-dependent behaviour of precast prestressed variable-section concrete girders is introduced, at the aim to furnish a valid procedure for practical purpose.

In particular the formulation includes the variation in time of both resistant sections and inertia along the beam axis and the variation of static scheme due to the elimination of provisional constraints and the introduction of permanent ones.

A correct design cannot neglect the above listed aspects, in order to obtain a realistic analysis of the behaviour with time of concrete.

2. Stess-strain state

Shrinkage and creep constitutive laws are assumed according to CEB-FIP Model Code 1990.

The shrinkage strains $\varepsilon_r(t,t_s)$ are expressed by

$$\varepsilon_r(t,t_s) = \varepsilon_s(f_{cm})\cdot\beta_{RH,T}\cdot\beta_s(t-t_s) \tag{1}$$

The creep coefficient can be calculated by

$$\varphi(t,t_s) = \varphi_0\cdot\beta_c(t-t_0) \tag{2}$$

The meaning of the above terms can be found in CEB (1991, 1993).

Due to the complexity of exact laws, for practical purpose simplifying hypotheses are usually introduced. In fact performing creep and shrinkage analyses by means of step-by-step procedures gives the most accurate solutions, but may involve some computational difficulties due to the overlarge number of calculations required (Pisani 1994, Fragiacomo *et al.* 2004, Gara *et al.* 2009).

Otherwise in practice acceptable results can be obtained by applying algebraic methods (Mola and Giussani 2003, Sassone and Chiorino 2005) which allow to perform one-step analyses. These methods are also characterized by a formal analogy with the associated elastic problem. In the following, algebraic methods are adopted, focusing on the Age-Adjusted Effective Modulus (AAEM) method (Bazant 1972, Bazant and Cedolin 2003).

In general the stress-strain relations can be expressed as follows

$$\varepsilon_c(t,t_0) = \frac{\sigma_c(t_0)}{E_c(t_0)}\cdot(1+\varphi(t,t_0)) + \frac{\sigma_c(t,t_0)-\sigma_c(t_0)}{E_c(t_0)}\cdot(1+\chi(t,t_0)\varphi(t,t_0)) - \varepsilon_r(t,t_s) \tag{3}$$

$$\sigma_c(t,t_0) = \varepsilon_c(t_0)E_c(t_0)\left(1-\frac{\varphi(t,t_0)}{1+\chi(t,t_0)\cdot\varphi(t,t_0)}\right) + (\varepsilon_c(t,t_0)-\varepsilon_c(t_0)+\varepsilon_r(t,t_s))\frac{E_c(t_0)}{1+\chi(t,t_0)\cdot\varphi(t,t_0)} \tag{4}$$

The ageing coefficient $\chi(t,t_0)$ is given by

$$\chi(t,t_0) = \frac{1}{1-\dfrac{R(t,t_0)}{E_c(t_0)}} - \frac{E_c}{E_c(t_0)\varphi(t,t_0)} \tag{5}$$

where $R(t,t_0)$ and E_c are respectively the relaxation function and the modulus of elasticity of concrete at 28 days (Chiorino 2005). The relaxation function can be obtained by the following semi-empirical expression (CEB 1991)

$$R(t,t_0) = \frac{1-0.008}{J(t,t_0)} - \frac{0.115}{J(t,t-1)}\left(\frac{J(t-\Delta,t_0)}{J(t,t_0+\Delta)}-1\right) \tag{6}$$

with $\Delta = (t-t_0)/2$, $J(t,t_0) = 1/E_c(t_0)+\varphi(t,t_0)/E_c$.

The ageing coefficient was firstly introduced by Bazant within the AAEM method, in fact the ratio $E_c(t_0)/(1+\chi(t,t_0)\cdot\varphi(t,t_0))$ represents the age-adjusted effective modulus.

The structure consists of prestressed concrete precast beams with pre-tensioned tendons. Precast beams are firstly joined by cast-in-place concrete in the vicinity of the supports and successively prestressed with post-tensioned tendons. The stress calculation in significant sections of the deck is carried out considering the elementary strip constituted by the individual precast beam, the cast-in-place concrete connection at supports and the top cast in-situ slab at mid-spans.

In order to generalize the proposed method, the following time steps are introduced:

– t_0 = age at which the precast beam is prestressed;
– t_1 = age at which, after the beams are placed, concrete is placed in-situ at supports;
– t_2 = age at which concrete at supports is prestressed and provisional restraints are replaced with permanent restraints;
– t_3 = age at which the slab is cast in-place at mid-spans;
– t_4 = age at which structural sections reach their final resistance and dead overloads are applied;
– t = age at which final forces and strains are calculated.

In each time step $(t_0,t_1),(t_1,t_2),(t_2,t_3),(t_3,t_4),(t_4,t)$ the analysis will be carried out taking into account a time t^+ corresponding to the upper limit of the step.

Fig. 1 shows the resistant sections referring to the just mentioned steps.

The composite beam is constituted by two main elements: the precast beam N and the in-situ concrete R. In the following $\varepsilon_N(t)$, $\varepsilon_R(t)$ and $\gamma_N(t)$, $\gamma_R(t)$ represent respectively the strains and the curvatures in correspondence of the centres of mass G_N and G_R; moreover $\varepsilon_{rN}(t_0,t)$ and $\varepsilon_{rR}(t_0,t)$ are the shrinkage strains in the two materials.

As to the cracking of the concrete slab, the condition is introduced that at the end of each time step the maximum tensile stresses do not exceed the tensile strength of concrete, that is all sections

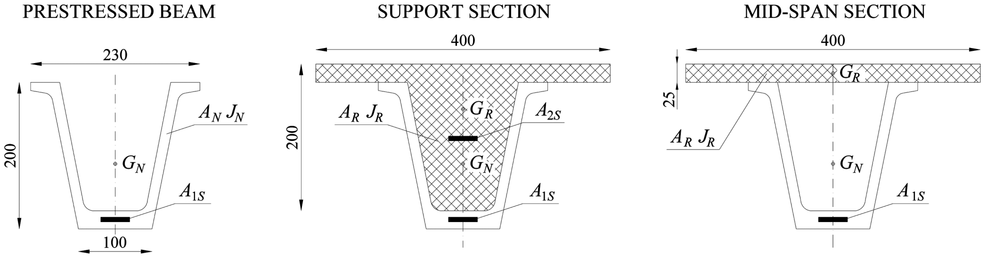

Fig. 1 Characteristic sections

are considered un-cracked. The slab-to-beam connection is realized through stud shear connectors able to absorb the longitudinal shear forces at the interface between the two elements, in order to guarantee a monolithic behaviour. Under this assumption sections remain plane to represent the linearity in the strain distribution on any section and at any time.

Therefore, in order to respect compatibility, at a generic time step Δt the strain-increment diagrams of the two parts constituting the composite section have to be parallel and the strain increments at the contact points of the precast beam with the in-situ concrete and with the prestressing tendons have to be equal.

With reference to the time interval (t_0, t_1), at time t_1 the prestressing force $N_i^{(0)}$ decreases as a result of shrinkage and creep and increases as a result of the bending moment due to the dead load of the beam $M_{g1}(\xi, t_0)$, ξ being the abscissa of the generic section. Moreover the simplifying hypothesis is introduced that the prestress losses due to the relaxation of the steel develop exclusively during prestressing (Mola 2000); so $N_i^{(0)}$ represents the force in the tendons at the stressing jacks less the losses due to the relaxation of the steel.

At the time interval (t_1, t_2) concrete is placed in-situ at supports; $M_{g2}(\xi, t_1)$ represents the bending moment due to this action. In this step the resistant section is represented exclusively by the precast beam (Fig. 2). At time t_2 the prestress force is given by (Mola 2000)

$$\begin{aligned} N_1(\xi, t_2) = {} & \left\{(1-D)\left(1-\frac{D\cdot\varphi_N(t_0,t_2)}{(1+D\cdot\chi_N(t_0,t_2)\varphi_N(t_0,t_2))}\right)\right\}\cdot N_1^{(0)} + M_{g1}(\xi,t_0)\frac{\dfrac{e_N^2}{r_N^2}D+\left(1+\dfrac{\varphi_N(t_0,t_2)(1-D)}{(1+D\cdot\chi_N(t_0,t_2)\varphi_N(t_0,t_2))}\right)}{e_N\cdot(1+e_N^2/r_N^2)} \\ & + M_{g2}(\xi,t_1)\frac{\dfrac{e_N^2}{r_N^2}D\left\{1+\dfrac{\varphi_N(t_1,t_2)(1-D)}{(1+D\cdot\chi_N(t_1,t_2)\varphi_N(t_1,t_2))}\right\}}{e_N\cdot(1+e_N^2/r_N^2)} - \frac{D\cdot E_N\cdot\varepsilon_{rN}(t_0,t_2)A_N}{(1+e_N^2/r_N^2)\cdot(1+D\cdot\chi_N(t_0,t_2)\cdot\varphi_N(t_0,t_2))} \end{aligned} \tag{7}$$

where $D = \dfrac{(1+e_N^2/r_N^2)}{(1+e_N^2/r_N^2)+(E_S A_{1S}/E_N A_N)^{-1}}$;

A_N and r_N are respectively the area and the radius of inertia of the cross section of the precast concrete beam; A_{1s} and e_N are respectively the area of prestressing tendons and the eccentricity of the prestressing resultant; E_N and E_s are respectively the moduli of elasticity of concrete and prestressing steel; χ_N is the ageing coefficient referred to the precast beam. In Eq. (7) the coefficient (1-D) is connected to the instantaneous reduction of the prestress force $N_1^{(0)}$ due to the shortening of concrete fibres at the steel-concrete interface.

From time t_2 two resistant sections can be identified: the precast beam with the in-situ concrete at supports (region a); the only precast beam (region b). At this instant the second prestressing $N_2^{(0)}$ is introduced in region a; more precisely $N_2^{(0)}$ represents the prestress force less the losses due to the relaxation of the steel.

At time t_3 the structure is completed by a cast-in-place concrete slab in region b; $M_{g3}(\chi, t_3)$ represents the corresponding bending moment.

At time t_4 all structural sections reach their final resistance and dead overloads are applied; $M_{sp}(\xi, t_4)$ represents the corresponding bending moment. From time t_4 the beam is so characterized only by composite sections (Fig. 3).

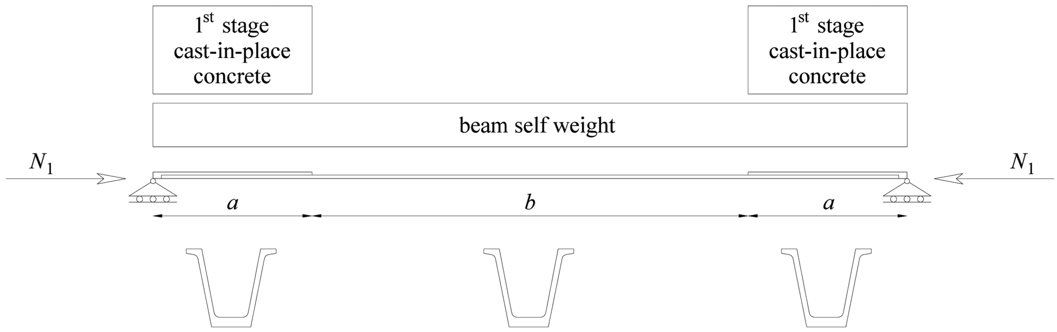

Fig. 2 Construction stages

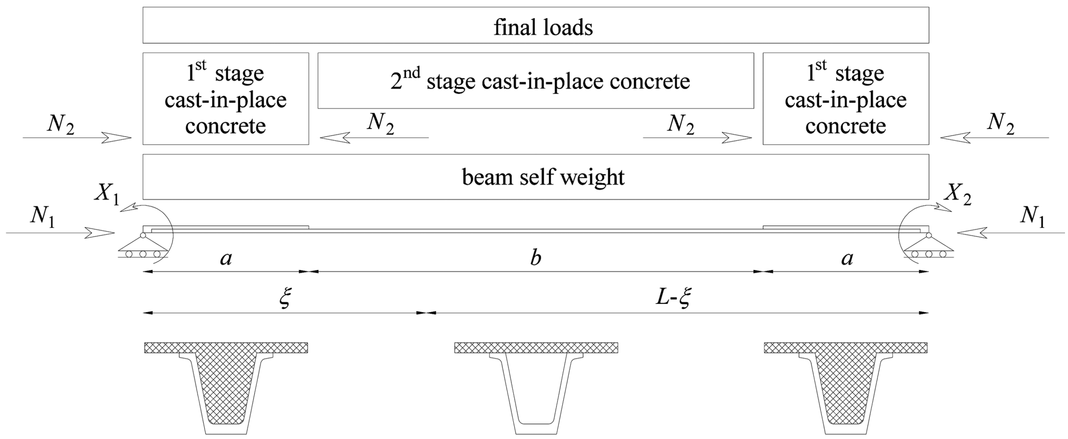

Fig. 3 Construction stages and actions

Finally, as to the casting technique, a stay-in-place formwork is used for slab casting and consequently the corresponding weight is included in the slab permanent load.

3. Connection of beams

The problem is herein simplified introducing the hypothesis that all beams are simultaneously connected through the formation of $n-1$ continuity restraints. The actual load condition in the m-th beam at a generic time $t > t_2$ is given by the superimposition of the external actions, the prestressing forces and the hyperstatic unknowns $X_{1m}(t_i)$, $X_{2m}(t_i)$ applied respectively at the right and left ends of the m-th beam. The bending moment due to the hyperstatic unknowns in the generic section can be expressed as

$$M_x(\xi, t_i) = \left(X_{1m}(t_i)\frac{L-\xi}{L} + X_{2m}(t_i)\frac{\xi}{L} \right) \qquad (t > t_2) \tag{8}$$

At time t_j the bending moment is given by

$$M_x(\xi,t_j)=M_x(\xi,t_i)+M_{\Delta x}(\xi,t_j)=M_x(\xi,t_i)+\left(\Delta X_{1m}(t_j)\frac{L-\xi}{L}+\Delta X_{2m}(t_j)\frac{\xi}{L}\right) \tag{9}$$

$\Delta X_{1m}(t_j)$ and $\Delta X_{2m}(t_j)$ being the variations of hyperstatic unknowns with respect to time t_i.

The bending moment $M_{\Delta x}(\xi,t_j)$ produces the following forces in the various elements of the composite section

$$\Delta N_N^{(\Delta x)}(\xi,t_j),\ \Delta N_R^{(\Delta x)}(\xi,t_j),\ \Delta M_N^{(\Delta x)}(\xi,t_j),\ \Delta M_R^{(\Delta x)}(\xi,t_j),\ \Delta N_{1S}^{(\Delta x)}(\xi,t_j),\Delta N_{2S}^{(\Delta x)}(\xi,t_j)$$

The above quantities can be easily obtained by applying balance and compatibility equations. Since these forces are equal to zero at the beginning of each step and reach the indicated values only at the end of the step, the corresponding viscoelastic strains of concrete can be estimated by

$$\begin{aligned}
\varepsilon_N^{(\Delta x)}(\xi,t_i,t_j)&=-\frac{\Delta N_N^{(\Delta x)}(\xi,t_j)}{E_N A_N}(1+\chi_N(t_i,t_j)\varphi_N(t_i,t_j))\\
\varepsilon_R^{(\Delta x)}(\xi,t_i,t_j)&=-\frac{\Delta N_R^{(\Delta x)}(\xi,t_j)}{E_R A_R}(1+\chi_R(t_i,t_j)\varphi_R(t_i,t_j))\\
\gamma_N^{(\Delta x)}(\xi,t_i,t_j)&=+\frac{\Delta M_N^{(\Delta x)}(\xi,t_j)}{E_N J_i}(1+\chi_N(t_i,t_j)\varphi_N(t_i,t_j))\\
\gamma_R^{(\Delta x)}(\xi,t_i,t_j)&=-\frac{\Delta M_R^{(\Delta x)}(\xi,t_j)}{E_R J_R}(1+\chi_R(t_i,t_j)\varphi_R(t_i,t_j))
\end{aligned} \tag{10}$$

while the strains of steel are given by

$$\varepsilon_{1S}^{(\Delta x)}(\xi,t_i,t_j)=-\frac{\Delta N_{1S}^{(\Delta x)}(\xi,t_j)}{E_S A_{1S}},\ \varepsilon_{2S}^{(\Delta x)}(\xi,t_i,t_j)=-\frac{\Delta N_{2S}^{(\Delta x)}(\xi,t_j)}{E_S A_{2S}} \tag{11}$$

4. Composite section

The present paragraph deals with the evaluation of the forces due to external actions, prestress and hyperstatic unknowns in each interval (t_i,t_j) following time t_2. The just mentioned forces are referred to the centres of mass of the two parts constituting the composite section.

In particular they can be divided into two groups. The first one is constituted by the forces $N_N(\xi,t_k)$, $M_N(\xi,t_k)$ and $N_R(\xi,t_k), M_R(\xi,t_k)$, acting respectively in the precast beam and in the in-situ concrete of the second stage. These forces already exist at the beginning of the specified step and produce only creep strains (that is without any elastic contribution).

The second one comprises the forces $\overline{N}_N(\xi,t_i)$ $\overline{M}_N(\xi,t_i)$ and $\overline{N}_R(\xi,t_i),\overline{M}_R(\xi,t_i)$, due to the loads applied at time t_i and involves the two parts of the concrete composite section. These forces produce viscoelastic strains, that is both the effects induced by creep and the corresponding elastic quantities occur.

Finally $N_1(\xi,t_i)$ and $N_2(\xi,t_i)$ are the tensile forces in the two centres of mass of the prestressing tendons already existing at the initial instant of the step, while $\overline{N}_1(\xi,t_i)$ and $\overline{N}_2(\xi,t_i)$ are the tensile forces produced by the external loads applied at the initial instant of the step (Fig. 4).

After determining the described forces, in the specified time interval it is possible to calculate the strains of the composite section materials.

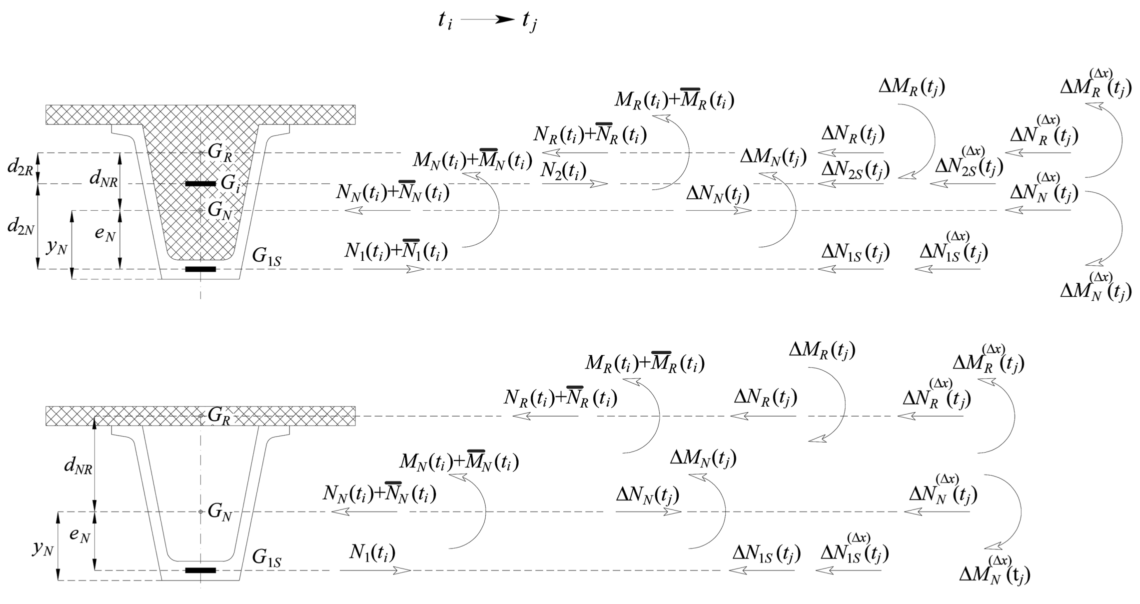

Fig. 4 Forces and migration forces

In order to respect compatibility conditions, a system of "migration forces" is introduced: $\Delta N_N(\xi,t_j)$ and $\Delta M_N(\xi,t_j)$ acting in the girder; $\Delta N_R(\xi,t_j)$ and $\Delta M_R(\xi,t_j)$ acting in the in-situ concrete; $\Delta N_{1S}(\xi,t_j)$ and $\Delta N_{2S}(\xi,t_j)$ acting in the prestressing tendons. This system of forces has to be self-balanced.

With reference to the symbols reported in Fig. 4, the total strains, including elastic, shrinkage, creep and hyperstatic unknowns contributions, in the time step (t_i,t_j) are given by

$$\varepsilon_N(\xi,t_i,t_j) = -\sum\frac{N_N(\xi,t_k)}{E_N A_N}\Delta\varphi_N(t_k,t_i,t_j) - \sum\frac{\overline{N}_N(\xi,t_i)}{E_N A_N}(1+\varphi_N(t_i,t_j)) +$$
$$+\frac{\Delta N_N(\xi,t_j)-\Delta N_N^{(\Delta x)}(\xi,t_j)}{E_N A_N}(1+\chi_N(t_i,t_j)\varphi_N(t_i,t_j)) + \varepsilon_{rN}(t_i,t_j)$$

$$\varepsilon_R(\xi,t_i,t_j) = -\sum\frac{N_R(\xi,t_k)}{E_R A_R}\Delta\varphi_R(t_k,t_i,t_j) - \sum\frac{\overline{N}_R(\xi,t_i)}{E_R A_R}(1+\varphi_R(t_i,t_j)) +$$
$$+\frac{\Delta N_R(\xi,t_j)-\Delta N_R^{(\Delta x)}(\xi,t_j)}{E_R A_R}(1+\chi_R(t_i,t_j)\varphi_R(t_i,t_j)) + \varepsilon_{rR}(t_i,t_j)$$

$$\gamma_N(\xi,t_i,t_j) = -\sum\frac{M_N(\xi,t_k)}{E_N J_N}\Delta\varphi_N(t_k,t_i,t_j) - \sum\frac{\overline{M}_N(\xi,t_i)}{E_N J_N}(1+\varphi_N(t_i,t_j)) +$$
$$+\frac{\Delta M_N(\xi,t_j)-\Delta M_N^{(\Delta x)}(\xi,t_j)}{E_N J_N}(1+\chi_N(t_i,t_j)\cdot\varphi_N(t_i,t_j))$$

$$\gamma_R(\xi,t_i,t_j) = -\sum\frac{M_R(\xi,t_k)}{E_R J_R}\Delta\varphi_R(t_k,t_i,t_j) - \sum\frac{\overline{M}_R(\xi,t_i)}{E_R J_R}(1+\varphi_R(t_i,t_j)) + \frac{\Delta M_R(\xi,t_j)-\Delta M_R^{(\Delta x)}(\xi,t_j)}{E_R J_R}(1+\chi_R(t_i,t_j)\cdot\varphi_R(t_i,t_j))$$

$$\varepsilon_{1S}(\xi,t_i,t_j) = -\sum \frac{\overline{N}_1(\xi,t_k)}{E_S A_{1S}} + \frac{\Delta N_{1S}(\xi,t_j) - \Delta N_{1S}^{(\Delta x)}(\xi,t_j)}{E_S A_{1S}}$$

$$\varepsilon_{2S}(\xi,t_i,t_j) = -\sum \frac{\overline{N}_2(\xi,t_k)}{E_S A_{2S}} + \frac{\Delta N_{2S}(\xi,t_j) - \Delta N_{2S}^{(\Delta x)}(\xi,t_j)}{E_S A_{2S}} \tag{12}$$

where $\Delta\varphi_N(t_k,t_i,t_j) = \varphi_N(t_k,t_j) - \varphi_N(t_k,t_i)$ and $\Delta\varphi_R(t_k,t_i,t_j) = \varphi_R(t_k,t_j) - \varphi_R(t_k,t_i)$.

In Eqs. (12) t_k represents the time at which loads preexisting at age t_i are applied. The corresponding forces include migration and hyperstatic unknowns effects.

The migration forces can be obtained by applying two balance equations and four compatibility equations involving the structural parts of the section

$$\begin{gathered}
\Delta N_N(\xi,t_j) = \Delta N_R(\xi,t_j) + \Delta N_{1S}(\xi,t_j) + \Delta N_{2S}(\xi,t_j) \\
\Delta M_N(\xi,t_j) = \Delta M_R(\xi,t_j) - \Delta N_N(\xi,t_j)\cdot d_{NR} + \Delta N_{1S}(\xi,t_j)\cdot(d_{NR}+e_N) + \Delta N_{2S}(\xi,t_j)\cdot d_{2R} \\
\varepsilon_R(\xi,t_i,t_j) - \varepsilon_N(\xi,t_i,t_j) = \gamma_N(\xi,t_i,t_j)\cdot d_{NR} \\
\gamma_R(\xi,t_i,t_j) = \gamma_N(\xi,t_i,t_j) \\
\varepsilon_{1s}(\xi,t_i,t_j) = \varepsilon_N(\xi,t_i,t_j) - \gamma_N(\xi,t_i,t_j)\cdot e_N \\
\varepsilon_{2s}(\xi,t_i,t_j) = \varepsilon_N(\xi,t_i,t_j) + \gamma_N(\xi,t_i,t_j)\cdot(d_{2N}-e_N)
\end{gathered} \tag{13}$$

In order to express creep strains as particular elastic strains, the following ideal or equivalent homogenization coefficients are introduced

$$\begin{gathered}
n_s = \frac{E_S}{E_N};\; n_R = \frac{E_R}{E_N}; \\
n_{S\Delta\varphi} = n_s \Delta\varphi_N(t_k,t_i,t_j);\; n_{S\varphi} = n_s(1+\varphi_N(t_i,t_j));\; n_{S\chi\varphi} = n_s(1+\chi_N(t_i,t_j)\varphi_N(t_i,t_j)); \\
n_{N\Delta\varphi} = \frac{\Delta\varphi_N(t_k,t_i,t_j)}{(1+\chi_N(t_i,t_j)\varphi_N(t_i,t_j))};\; n_{N\varphi} = \frac{(1+\varphi_N(t_i,t_j))}{(1+\chi_N(t_i,t_j)\varphi_N(t_i,t_j))}; \\
n_{R\Delta\varphi} = \frac{\Delta\varphi_R(t_k,t_i,t_j)}{(1+\chi_R(t_i,t_j)\varphi_R(t_i,t_j))};\; n_{R\varphi} = \frac{(1+\varphi_R(t_i,t_j))}{(1+\chi_R(t_i,t_j)\varphi_R(t_i,t_j))}; \\
n_{R\chi\varphi} = n_R \frac{(1+\chi_N(t_i,t_j)\varphi_N(t_i,t_j))}{(1+\chi_R(t_i,t_j)\varphi_R(t_i,t_j))}
\end{gathered} \tag{14}$$

Introducing the following symbols

$$\begin{gathered}
\mathbf{N}_N = \sum N_N(\xi,t_k)\cdot n_{N\Delta\varphi} + \sum \overline{N}_N(\xi,t_i)\cdot n_{N\varphi} + \Delta N_N^{(\Delta x)}(\xi,t_j); \\
\mathbf{N}_R = \sum N_R(\xi,t_k)\cdot n_{R\Delta\varphi} + \sum \overline{N}_R(\xi,t_i)\cdot n_{R\varphi} + \Delta N_R^{(\Delta x)}(\xi,t_j) \\
\mathbf{M}_N = \sum M_N(\xi,t_k)\cdot n_{N\Delta\varphi} + \sum \overline{M}_N(\xi,t_i)\cdot n_{N\varphi} + \Delta M_N^{(\Delta x)}(\xi,t_j) \\
\mathbf{M}_R = \sum M_R(\xi,t_k)\cdot n_{R\Delta\varphi} + \sum \overline{M}_R(\xi,t_i)\cdot n_{R\varphi} + \Delta M_R^{(\Delta x)}(\xi,t_j) \\
\mathbf{N}_{1S} = \sum \overline{N}_1(\xi,t_i) + \Delta N_{1S}^{(\Delta x)}(\xi,t_j) \qquad \mathbf{N}_{2S} = \sum \overline{N}_2(\xi,t_i) + \Delta N_{2S}^{(\Delta x)}(\xi,t_j) \\
\mathbf{N}_{rN} = \varepsilon_{rN}(t_i,t_j)\frac{E_N A_N}{1+\chi_N(t_i,t_j)\varphi_N(t_i,t_j)} \qquad \mathbf{N}_{rR} = \varepsilon_{rR}(t_i,t_j)\frac{E_R A_R}{(1+\chi_R(t_i,t_j)\varphi_R(t_i,t_j))}
\end{gathered} \tag{15}$$

the migration forces can be expressed as

$$
\begin{cases}
\Delta M_N(\xi,t_j) = \dfrac{(\mathbf{M}_N H_3 + (\mathbf{N}_N - \mathbf{N}_{rN})(1+H_1) - (\mathbf{N}_{1S}+\mathbf{N}_{2S}) - (-\mathbf{N}_{rR}+\mathbf{N}_R))H_6}{H_1H_4+H_3H_6} + \\
\qquad + \dfrac{(-\mathbf{M}_N(1-H_4) + (\mathbf{N}_{rN}-\mathbf{N}_N)(H_6+d_{NR}) + \mathbf{M}_R + \mathbf{N}_{1S}\cdot(d_{NR}+e_N) + \mathbf{N}_{2S}d_{2R})H_1}{H_1H_4+H_3H_6} \\
\Delta N_N(\xi,t_j) = \dfrac{(\mathbf{M}_N H_3 + (\mathbf{N}_N - \mathbf{N}_{rN})(1+H_1) - (\mathbf{N}_{1S}+\mathbf{N}_{2S}) - (-\mathbf{N}_{rR}+\mathbf{N}_R))H_4}{H_1H_4+H_3H_6} + \\
\qquad - \dfrac{(-\mathbf{M}_N(1-H_4) + (\mathbf{N}_{rN}-\mathbf{N}_N)(H_6+d_{NR}) + \mathbf{M}_R + \mathbf{N}_{1S}\cdot(d_{NR}+e_N) + \mathbf{N}_{2S}d_{2R})H_3}{H_1H_4+H_3H_6} \\
\Delta N_R(\xi,t_j) = -\mathbf{N}_{1S} - \mathbf{N}_{2S} + n_{S\chi\varphi}(\mathbf{N}_N-\mathbf{N}_{rN})(\mu_{1S}+\mu_{2S}) + \dfrac{n_{S\chi\varphi}}{r_N^2}\mathbf{M}_N(-\mu_{1S}e_N + \mu_{2S}d_{2N} - \mu_{2S}e_N) + \\
\qquad + \Delta N_N(\xi,t_j)(1-\mu_{1S}n_{S\chi\varphi} - \mu_{2S}n_{S\chi\varphi}) + \dfrac{n_{S\chi\varphi}}{r_N^2}\Delta M_N(\xi,t_j)(\mu_{1S}e_N - \mu_{2S}d_{2N} + \mu_{2S}e_N) \\
\Delta M_R(\xi,t_j) = \Delta M_N(\xi,t_j)\left(H_4 + \dfrac{\mu_R n_{R\chi\varphi} r_R^2}{r_N^2}\right) - \Delta N_N(\xi,t_j)H_6 - \mathbf{N}_{1S}(d_{NR}+e_N) - \mathbf{N}_{2S}d_{2R} + \\
\qquad + (\mathbf{N}_N - \mathbf{N}_{rN})(H_6+d_{NR}) + \mathbf{M}_N\left(1 - \dfrac{\mu_R n_{R\chi\varphi} r_R^2}{r_N^2} - H_4\right) \\
\Delta N_{1S}(\xi,t_j) = \mathbf{N}_{1S} - \mu_{1S}n_{S\chi\varphi}(\mathbf{N}_N-\mathbf{N}_{rN}) + \dfrac{\mu_{1S}n_{S\chi\varphi}e_N}{r_N^2}\mathbf{M}_N + \mu_{1S}n_{S\chi\varphi}\Delta N_N(\xi,t_j) + \\
\qquad - \dfrac{\mu_{1S}n_{S\chi\varphi}e_N}{r_N^2}\Delta M_N(\xi,t_j) \\
\Delta N_{2S}(\xi,t_j) = \mathbf{N}_{2S} - \mu_{2S}n_{S\chi\varphi}(\mathbf{N}_N-\mathbf{N}_{rN}) - \dfrac{\mu_{2S}n_{S\chi\varphi}}{r_N^2}(d_{2N}-e_N)\mathbf{M}_N + \mu_{2S}n_{S\chi\varphi}\Delta N_N(\xi,t_j) + \\
\qquad + \dfrac{\mu_{2S}n_{S\chi\varphi}}{r_N^2}(d_{2N}-e_N)\Delta M_N(\xi,t_j)
\end{cases}
\tag{16}
$$

where

$$H_1 = -1 + n_{S\chi\varphi}(\mu_{1S}+\mu_{2S}) + n_{R\chi\varphi}\cdot\mu_R\,;$$

$$H_3 = \frac{1}{r_N^2}\cdot(-\mu_{1S}n_{S\chi\varphi}e_N + \mu_{2S}n_{S\chi\varphi}(d_{2N}-e_N) - \mu_R n_{R\chi\varphi}d_{NR})\,;$$

$$H_4 = 1 + \frac{1}{r_N^2}\cdot(\mu_{1S}n_{S\chi\varphi}e_N(d_{NR}+e_N) - \mu_{2S}n_{S\chi\varphi}d_{2R}(d_{2N}-e_N) - \mu_R\cdot n_{R\chi\varphi}\cdot r_R^2)\,;$$

$$H_6 = +n_{S\chi\varphi}(\mu_{1S}(d_{NR}+e_N) + \mu_{2S}d_{2R}) - d_{NR}\,;$$

$$\mu_{1S} = \frac{A_{1S}}{A_N};\quad \mu_{2S} = \frac{A_{2S}}{A_N};\quad \mu_R = \frac{A_R}{A_N};\quad r_R^2 = \frac{J_R}{A_R};\quad r_N^2 = \frac{J_N}{A_N} \tag{17}$$

The system of equation in six unknowns (13) has been solved by the software Mathematica. The expressions so obtained have been also implemented in MATLAB, in order to facilitate the application of the procedure for practical purpose.

At each step it is then possible to determine the forces acting in the different parts of the composite section and the corresponding strains.

The migration quantities depend on the hyperstatic unknowns. The hyperstatic unknowns $\Delta X_{1m}(t_j)$ and $\Delta X_{2m}(t_j)$ can be calculated by solving the following system of compatibility equations

$$(\theta_{02}(t_i,t_j))_m = (\theta_{01}(t_i,t_j))_{m+1} \qquad (m=1\ldots n-1) \tag{18}$$

$\theta_{01}(t_i,t_j)$ and $\theta_{02}(t_i,t_j)$ being the rotations in the extreme sections of the generic m-th beam at the end of each time step

$$\theta_{01}(t_i,t_j) = \int_0^L \gamma_N(\xi,t_i,t_j)\frac{L-\xi}{L}d\xi;\ \theta_{02}(t_i,t_j) = \int_0^L \gamma_N(\xi,t_i,t_j)\frac{\xi}{L}d\xi \tag{19}$$

It can be noted that Eq. (18) express the equality of rotations in two contiguous sections respectively of the m-th and (m+1)-th beams; that is the hyperstatic unknowns are those moments whose application at the ends of the released beams allows to satisfy the compatibility conditions of the beam-end rotations.

In this study temperature effects are neglected since a temperature difference between the slab and the precast beam leads to an overall reduction of the maximum stresses of the beam (at the bottom fibre). However they can be easily taken into account according to CEN (2001).

The above exposed principles are applied in order to determine the stress-strain state in the beam sections with reference to different construction stages.

4.1 Time step (t_2, t_3)

At time t_2 the second prestress is transferred to concrete in region a. Prestress consequently involves only the regions of the beam completed with cast-in-place concrete in the first stage. At the step under examination both the creep strains due to preexisting actions and the instantaneous elastic and creep strains produced by the second prestress and the hyperstatic unknowns are present; obviously shrinkage effects develop in the two parts of the composite section. Since external constraints do not avoid the elastic shortenings due to the second stage prestress in region a, region b is not affected by the elastic strains produced by this coercion.

At time t_2, in region a the forces due to the second prestress are given by

$$\overline{N}_N(\xi,t_2) = N_2(\xi,t_2)\frac{A_N}{A_i};\ \overline{N}_R(\xi,t_2) = N_2(\xi,t_2)n_R\frac{A_R}{A_i};\ \overline{N}_1(\xi,t_2) = N_2(\xi,t_2)n_S\frac{A_{1S}}{A_i} \tag{20}$$

with $A_i = A_N + n_R A_R + n_S A_{1S}$.

Thus at time t_3 it is possible to calculate the migration forces and the hyperstatic unknowns by applying respectively Eqs. (16) and (18).

4.2 Time step (t_3, t_4)

At time t_3, the slab is placed in-situ in the central region of beams (region b); $M_{g3}(\xi,t_3)$ is the corresponding bending moment.

In region *a*, where a composite section is already present, the forces due to $M_{g3}(\xi,t_3)$ are

$$\overline{N}_N(\xi,t_3)=\frac{S_N}{J_i}M_{g3}(\xi,t_3);\ \overline{M}_N(\xi,t_3)=\frac{J_N}{J_i}M_{g3}(\xi,t_3) \tag{21}$$

$$\overline{N}_R(\xi,t_3)=\frac{n_R\cdot S_R}{J_i}M_{g3}(\xi,t_3);\ \overline{N}_1(\xi,t_4)=\frac{n_s S_{A1}}{J_i}M_{g3}(\xi,t_4);\ \overline{N}_2(\xi,t_4)=0$$

where S_N and S_R are the static moments of the two parts of the composite section with respect to the barycentric axis of the homogenised section; S_{A1} is the static moment of the first prestressing tendons with respect to the barycentric axis of the homogenised section; J_i is the inertial moment of the homogenised section with respect to its barycentric axis.

4.3 Time step (t_4, t)

The slab in region *b* contributes to the section resistance. Therefore the beam is subject to another variation of inertia. Moreover the hypothesis is introduced that dead overloads are applied at the beginning of this interval; $M_{SP}(\xi,t_4)$ is the corresponding bending moment.

In region *a* the forces acting at time t_4 and producing viscoelastic strains in concrete and elastic strains in prestressing tendons are

$$\overline{N}_N(\xi,t_4)=\frac{S_N}{J_i}M_{sp}(\xi,t_4);\quad \overline{M}_N(\xi,t_4)=\frac{J_N}{J_i}M_{sp}(\xi,t_4);$$

$$\overline{N}_R(\xi,t_4)=\frac{n_R\cdot S_R}{J_i}M_{sp}(\xi,t_4)\quad \overline{M}_R(\xi,t_4)=n_R\frac{J_R}{J_i}M_{sp}(\xi,t_4); \tag{22}$$

$$\overline{N}_1(\xi,t_4)=n_S\frac{S_{A1}}{J_i}M_{sp}(\xi,t_4)\quad \overline{N}_2(\xi,t_4)=0$$

At time *t* the final forces are

$$\begin{aligned}
M_N(\xi,t)&=\Sigma\overline{M}_N(\xi,t_4)+\Sigma M_N(\xi,t_4)+\Delta M_N(\xi,t)+\Delta M_N^{(\Delta x)}(\xi,t)\\
N_N(\xi,t)&=\Sigma\overline{N}_N(\xi,t_4)+\Sigma N_N(\xi,t_4)+\Delta N_N(\xi,t)+\Delta N_N^{(\Delta x)}(\xi,t)\\
M_R(\xi,t)&=\Sigma\overline{M}_R(\xi,t_4)+\Sigma M_R(\xi,t_4)+\Delta M_R(\xi,t)+\Delta M_R^{(\Delta x)}(\xi,t)\\
N_R(\xi,t)&=\Sigma\overline{N}_R(\xi,t_4)+\Sigma N_R(\xi,t_4)+\Delta N_R(\xi,t)+\Delta N_R^{(\Delta x)}(\xi,t)\\
N_1(\xi,t)&=\Sigma\overline{N}_1(\xi,t_4)+\Sigma N_1(\xi,t_4)+\Delta N_{1S}(\xi,t)+\Delta N_{1S}^{(\Delta x)}(\xi,t)\\
N_2(\xi,t)&=\Sigma\overline{N}_2(\xi,t_4)+\Sigma N_2(\xi,t_4)+\Delta N_{2S}(\xi,t)+\Delta N_{2S}^{(\Delta x)}(\xi,t)
\end{aligned} \tag{23}$$

The same forces act in region *b*, obviously with different values of the quantities S_R and J_R.

5. Numerical application

The proposed method has been utilized in order to evaluate the stress-strain state of the viaduct "Quattroquerce", built on the "A3" Salerno-Reggio Calabria (Fig. 5). The viaduct is constituted by

Fig. 5 Viaduct “Quattroquerce”

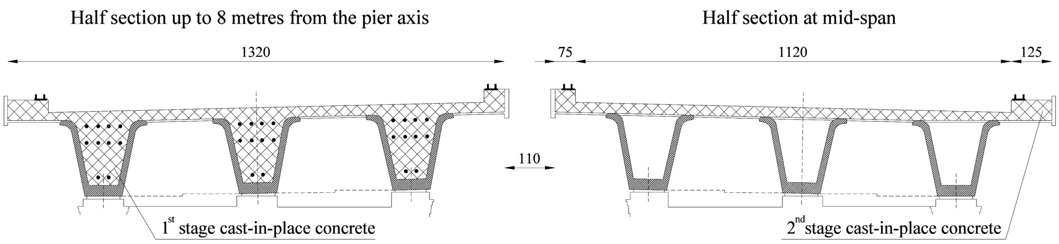

Fig. 6 Sections of the viaduct respectively up to 8 metres from the pier axis and at mid-span

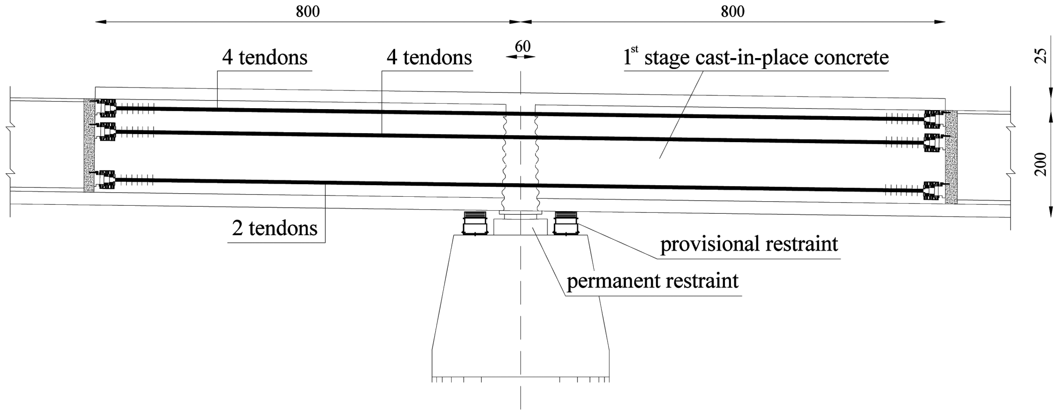

Fig. 7 Longitudinal section of the girder in correspondence of the pier

Table 1 Structural characteristics of the composite section

	R_{ck} [MPa]	A [cm^2]	J [cm^4]	RH%	T	Prestress force [kN]
Prestressed beam	55	8587	39886500	50	20°	28690
Cast-in-place concrete at supports	40	30184	103871200	50	20°	11330
Slab	35	10000	520834	50	20°	

15 spans, the first and last of which are 33.7 m in length and the others 38.00 m. The girder is characterized by precast prestressed beams, with pre-tensioned tendons placed at an interval of 4.00 m. The height of the beams is 2.00 m, the width of the slab is 25 cm. Fig. 6 shows two characteristic transversal sections of the girder, in correspondence respectively of the pier and the mid-span. Fig. 7 illustrates the longitudinal section of the girder in correspondence of the pier. The structural characteristics of the girder are reported in Table 1, while the values of the main loads are

Table 2 Main loads

Prestressed beam self-weight [kN/m]	Cast-in-place concrete at supports self-weight [kN/m] (1st stage)	Slab self-weight [kN/m] (2nd stage)	Dead overloads [kN/m]
22	76	29	23

Table 3 Main time steps

Casting of beams	1st stage cast-in-place concrete	Post-tensioning	2nd stage cast-in-place concrete	Realization of finishes	Under service		
t_0=3 days	t_1=72 days	t_2=86 days	t_3=200 days	t_4=214 days	t_5=300 days	t_6=665 days	t_7=4000 days


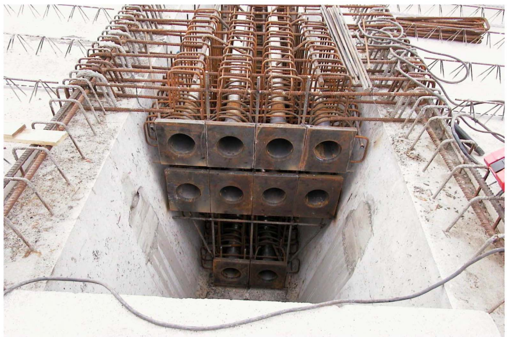

Fig. 8 Anchorage devices of tendons before post-tensioning

summarized in Table 2. The time steps considered in the analysis are reported in Table 3.

Fig. 8 provides two images of the anchorage devices of tendons, at a distance of 8.00 m from the pier axis, before in place post-tensioning.

The results of the analysis are shown with reference to a final time equal to $t_7 = 4000$ days. In fact, taking into account that CEB-FIB model is characterized by an asymptotic limit value of strain for $t \rightarrow \infty$, adopting $t_0 = 3$ days, the solution for $t > 4000$ days can be considered practically constant in time. Contrarily more recent models, such as the B3 model, are characterized by a linear law of strain (in logarithmic scale) for $t > 1000$ days (Bazant 1995, Gardner and Lockman 2001). However the above prediction models are validated on the basis of experimental data referring to a time $t = 3$ years (Data Base Rilem), while a reliable determination of the final value of the stress-strain state would require measurements of at least 5 years duration, which are not available in literature. Therefore, since for $t = 3$ years CEB-FIB and B3 models furnish comparable results, in this numerical application the CEB-FIB model is applied and the analysis refers to a final time $t_7 = 4000$ days (Bazant 2001, Ceccoli *et al.* 2000).

Since the final stress state is considerably influenced by the time t_2, at which the structural continuity is realized, two extreme cases are firstly analyzed, corresponding to a realization time T_R of the structure equal respectively to 30 days (theoretical value) and 2 years (upper limit). Fig. 9 shows a comparison in terms of stresses of the results so obtained. The results are expressed separating the effects due to prestressing and dead loads from the effects produced by shrinkage and creep. In fact the first ones do not depend on time, while the second ones are considerably influenced by the realization time of the viaduct. In particular as the realization time T_R decreases,

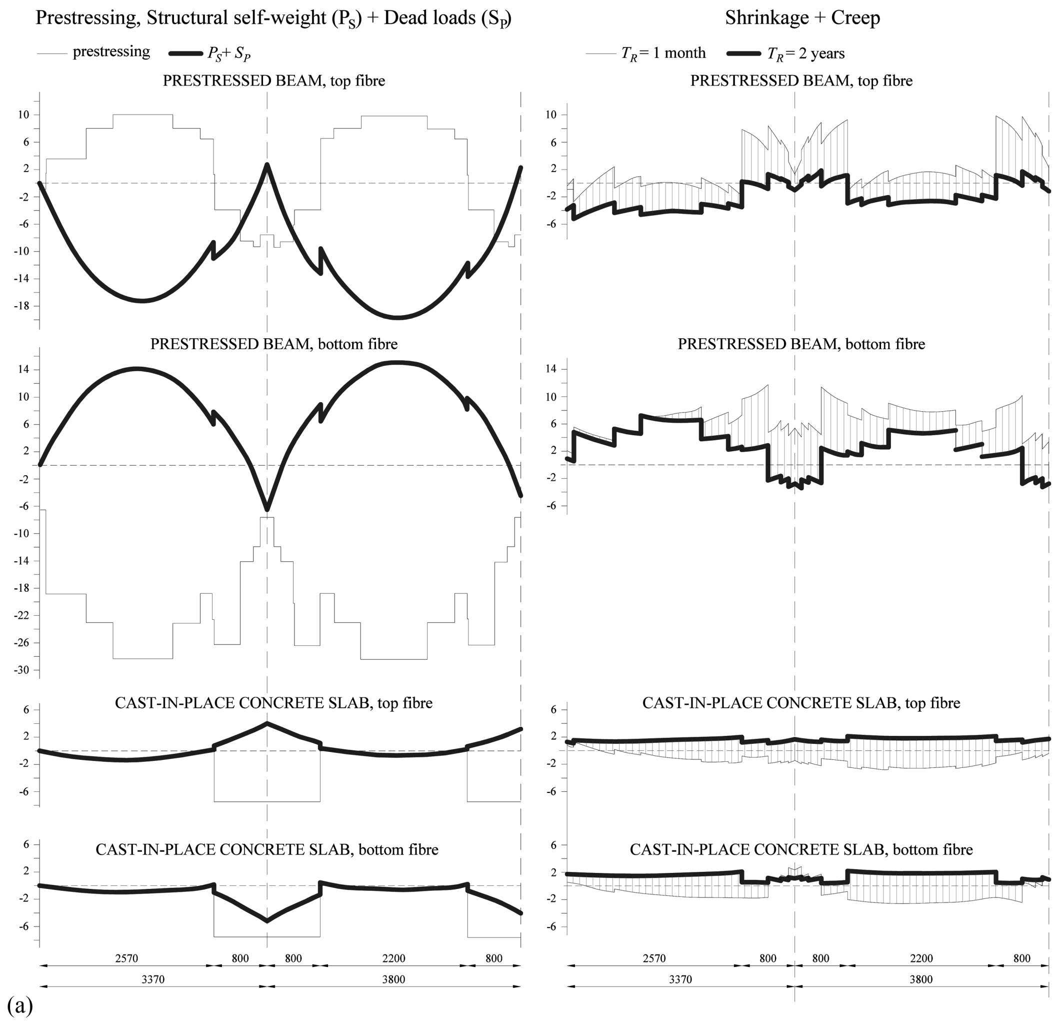

(a)

Realization time	Casting of beams	1st stage cast-in-place concrete	Post-tensioning	2nd stage cast-in-place concrete	Realization of finishes	
T_R=1 month	t_0=3 days	t_1=4 days	t_2=18 days	t_3=19 days	t_4=30 days	t=4000 days
T_R=2 years	t_0=3 days	t_1=586 days	t_2=600 days	t_3=716 days	t_4=730 days	t=4000 days

(b)

Fig. 9 (a) Final stress states [MPa] at time $t = 4000$ days at the top and bottom fibres of the precast beam and of the slab in correspondence of (b) two hypotheses of construction stages

axial stresses due to viscous effects increase in the prestressed beam, reducing the compressive stresses both at mid-spans and at supports. This is due to the partial reduction of the stresses produced by the realization of continuity restraints. Otherwise, as time T_R decreases, compressive stresses in the additional cast-in-place slab increase, as a consequence of creep. Finally it is worth noting that discontinuities in the diagram of prestressing stresses along the beam are due to the geometric distribution of tendons.

Fig. 10 shows the evolution in time of the stress state at the top and bottom fibres of the precast

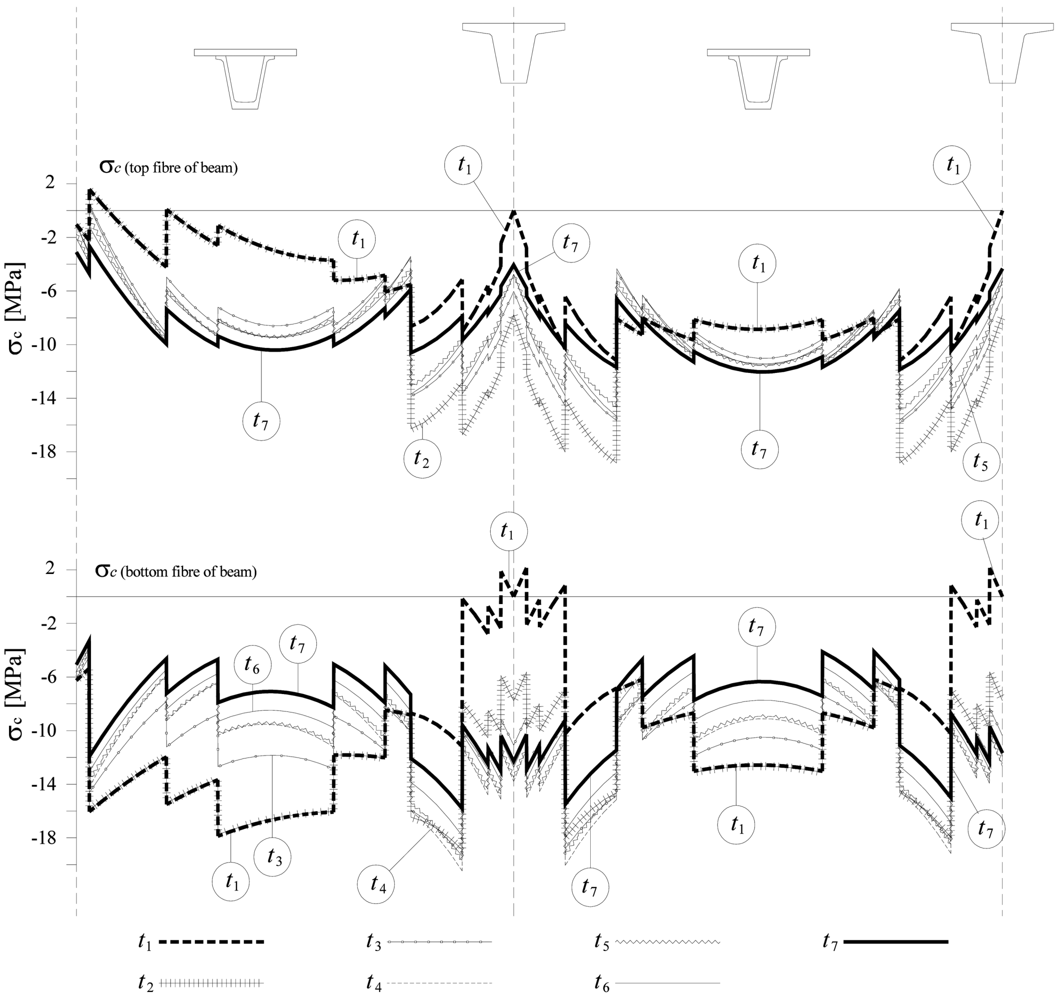

Fig. 10 Evolution in time of the stress state at the top and bottom fibres of the precast beam

beam according to the time steps summarized in Table 3 and with reference to the first two spans of the viaduct, characterized by the highest load conditions. At each time taken into account, the stress diagram is discontinuous along the beam axis as a consequence of the variation of both section properties and prestressing force (Fig. 9). Moreover at each time step stresses are evaluated in terms of increments with respect to the previous instant. It emerges that creep and shrinkage effects due to both permanent loads and variation of static scheme, developing from time t_3 to time t_7, significantly affect the values of stresses along the span lengths. In particular at the mid of the first span the just mentioned effects lead to a reduction of stresses equal to about 38%.

Fig. 11 also shows the final stresses at time $t_7 = 4000$ days at the top and bottom fibres of both the prestressed beam and the slab. It can be noted that all sections are compressed or slowly tense, in accordance with the hypothesis of un-cracked condition.

In order to validate the proposed procedure, the just described results have been compared with the values obtained by approximate estimations of creep and shrinkage effects. More precisely, for

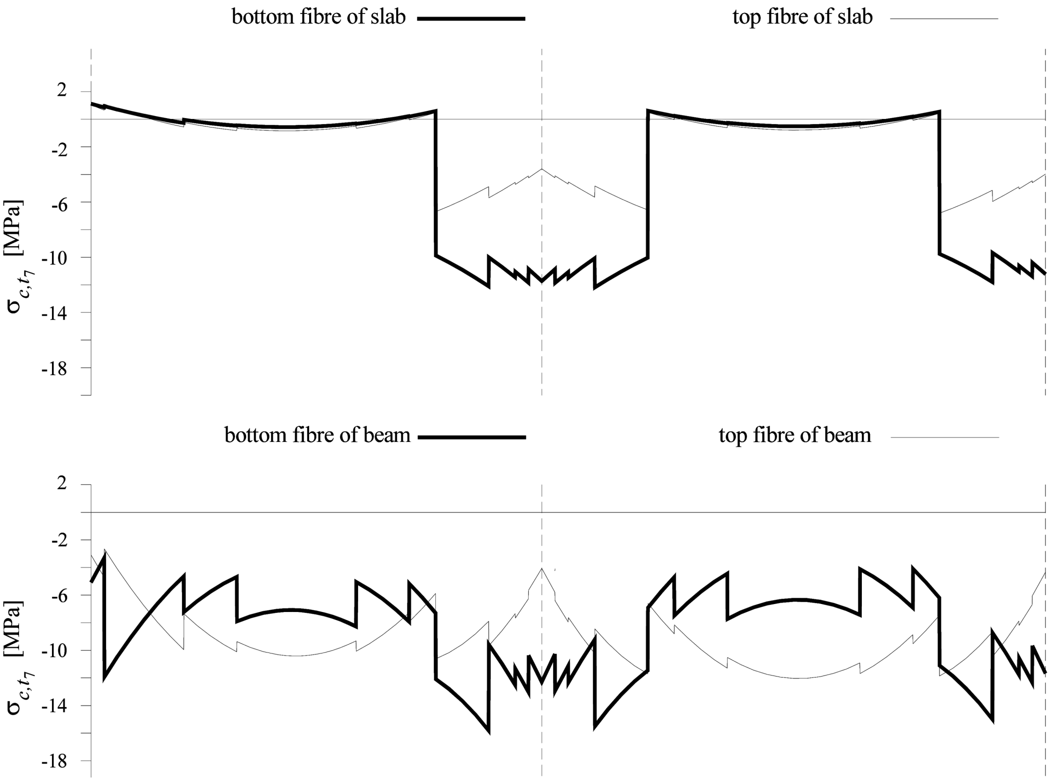

Fig. 11 Stresses at the extreme fibres of the slab and of the precast beam at time $t_7 = 4000$ days

creep and shrinkage due to permanent loads, an approximate evaluation has been obtained by assuming that 30% of the corresponding effects develop before casting the slab (t_1 or t_3), 30% before time t_4 and the residual 40% before time t_5. Similarly shrinkage effects due to the replacement of provisional restraints with permanent restraints have been approximately taken into account by assuming the final stresses equal to the sum of 1/3 of the stresses calculated referring to the static scheme with provisional restraints and 2/3 of the stresses obtained referring to the static scheme with permanent restraints (Petrangeli 1993, Neville *et al.* 1983, Gilbert 1988). The approximate values of the stresses so obtained are bigger (+10-15%) than the ones accurately calculated by the proposed procedure, but allow to asses the correctness of the method.

6. Conclusions

The study herein carried out shows that shrinkage and creep considerably affect the behaviour of composite prestressed structures, regarding both stress and strain states.

Construction techniques, geometrical and mechanical characteristics of sections, applied loads, rheological non-homogeneities, post-poned restraints and consequently variations of static schemes, contribute to make structures widely sensitive to delayed strains. Therefore the prediction of the behaviour with time of concrete structures should be carried out taking into account all the significant parameters, in order to obtain values of unknown variables as close as possible to the real ones.

In the present paper a procedure has been proposed in order to evaluate the long-term stress-strain state of prestressed composite beams, taking into account structural effects due to shrinkage, creep and static scheme modifications. The method is based on the introduction of equivalent moduli, depending on the viscous and elastic features of materials. The results show that creep and shrinkage effects due to both permanent loads and variation of static scheme significantly affect the values of stresses along the span lengths, leading to a reduction/increasing of stresses up to 38%.

The compact formulation herein introduced is very suitable for design applications since it allows to check the stress-strain state of the structure from the preliminary phase to the service one.

References

Bae, H.G., Oliva, M.G. and Bank, L.C. (2010), "Obtaining optimal performance with reinforcement-free concrete highway bridge decks", *Eng. Struct.*, **32**(8), 2300-2309.

Bazant, Z.P. (1972), "Prediction of concrete creep effects using age-adjusted effective modulus method", *ACI J.,* **69**(4), 212-217.

Bazant, Z.P. (1995), "Creep and shrinkage prediction model for analysis and design of concrete structures - model B3", *Mater. Struct.*, **28**(6), 357-365.

Bazant, Z.P. (2000), "Structural stability", *Int. J. Solids Struct.*, **37**(1-2), 55-67.

Bazant, Z.P. (2001), "Prediction of concrete creep and shrinkage: past, present and future", *Nucl. Eng. Des.*, **203**(1), 27-38.

Bazant, Z.P. and Cedolin, L. (2003), *Stability of structures. Elastic, Inelastic, Fracture and Damage Theories*, Dover Publications, Inc., Mineola, New York, 584-632.

CEB (1991), *CEB-FIP Model Code 1990*, CEB Bulletin d'Information N° 203/205, Thomas Telford, London.

CEB (1993), *CEB-FIP Model Code 1990*, CEB Bulletin d'Information N° 215, Thomas Telford, London.

Ceccoli, C, Mazzotti, C. and Savoia, M. (2000), "Analisi statistica per la validazione dei modelli di previsione delle deformazioni viscose del calcestruzzo", *13° Congresso C.T.E.*, Pisa, 9-11 (in Italian).

CEN (2001), "Eurocode 2. Design of concrete structures - Part 1: General rules and rules for buildings", EN 1992-1.

Chiorino, M.A. (2005), "A rational approach to the analysis of creep structural effects", *Shrinkage and Creep of Concrete,* N. J. Gardner and J. Weiss Eds., ACI SP-227, 107-141.

Dezi, L. and Tarantino, A.M. (1991), "Time-dependent analysis of concrete structures with variable structural system", *ACI Mater. J.*, **88**(3), 320-324.

Dezi, L., Gara, F. and Leoni, G. (2006), "Construction sequence modelling of continuous steel-concrete composite bridge decks", *Steel Compos. Struct.*, **6**(2), 123-138.

Fiore, A. and Monaco, P. (2009), "POD-based representation of the alongwind equivalent static force for long-span bridges", *Wind Struct.*, **12**(3), 239-257.

Fragiacomo, M., Amadio, C. and Macorini, L. (2004), "Finite-element model for collapse and long-term analysis of steel-concrete composite beams", *J. Struct. Eng.-ASCE*, **130**(3), 489-497.

Gara, F., Leoni, G. and Dezi, L. (2009), "A beam finite element including shear lag for the time-dependent analysis of steel-concrete composite decks", *Eng. Struct.*, **31**(8), 1888-1902.

Gardner, N.J. and Lockman, M.J. (2001), "Design provisions for drying shrinkage and creep of normal-strength concrete", *ACI Mater. J.*, **98**(2), 159-167.

Ghali, A. (1989), "Stress and strain analysis in pre-stressed concrete: a critical review", *PCI J.*, **34**(6), 80-97

Gilbert, R.I. (1988), *Time effects in concrete structures*, Elsevier.

Gilbert, R.I. (1989), "Time-dependent analysis of composite steel-concrete sections", *J. Struct. Eng.*, ASCE, **115**(11), 2687-2705.

Kwak, H.G. and Seo, Y.J. (2002), "Shrinkage cracking at interior supports of continuous pre-cast pre-stresse concrete girder bridges", *Constr. Build. Mater.*, **16**(1), 35-47.

Kwak, H.G., Seo, Y.J. and Jung, C.M. (2000), "Effects of the slab casting sequences and the drying shrinkage of concrete slabs on the short-term and long-term behaviour of composite steel box girder bridges", *Eng. Struct.*, **22**(11), 1453-1466.
Marì, A.R., Mirambell, E. and Estrada, I. (2003), "Effects of construction process and slab prestressing on the serviceability behaviour of composite bridges", *J. Constr. Steel Res.,* **59**(2), 135-163.
Mola, F. (1986), "Analisi generale in fase viscoelastica lineare di strutture e sezioni a comportamento reologico non omogeneo", *Studi e Ricerche – Vol. 8*, Graduate School in Concrete Structures, Fratelli Pesenti, Politecnico di Milano, Italy.
Mola, F. (1988), "Studio del comportamento a lungo termine di strutture caratterizzate da disomogeneità reologiche distribuite lungo l'asse e nelle sezioni trasversali", *Studi e Ricerche - Vol. 10*, Graduate School in Concrete Structures, Fratelli Pesenti, Politecnico di Milano, Italy.
Mola, F. (2000), "Gli effetti della viscosità nei ponti a travata continua. Evoluzione degli schemi strutturali", *Atti del corso di aggiornamento sui ponti e viadotti*, Politecnico di Milano, Pitagora ed., Bologna, (in Italian).
Mola, F. and Giussani, F. (2003), "Service stage behaviour of composite bridges", *Proceedings of the 3rd International Conference on New Dimensions in Bridges, Flyovers, Overpasses & Elevated Structures*, 9-10, Malaysia.
Neville, A.M., Dilger, W.H. and Brooks, J.J. (1983), *Creep of plain and structural concrete*, Construction Press, London.
Petrangeli, M.P. (1993), *Progettazione e Costruzione di Ponti*, Masson Editoriale Esa, Italy.
Pisani, M.A. (1994), "Numerical analysis of creep problems", *Comput. Struct.*, **51**(1), 57-63.
Sassone, M. and Chiorino, M.A. (2005), "Design aids for the evaluation of creep induced structural effects", *Shrinkage and Creep of Concrete,* N. J. Gardner and J. Weiss Eds., ACI SP-227, 239-259.

CC